

ARTICLE



Anterior segment optical coherence tomography characteristics of conjunctival papilloma as compared to papilliform ocular surface squamous neoplasia

Wathanee Sripawadkul^{1,2}, Rayan Abou Khzam¹, Vincent Tang¹, Mike Zein¹, Sander R. Dubovy^{1,3}, Anat Galor^{1,4} and Carol L. Karp¹✉

© The Author(s), under exclusive licence to The Royal College of Ophthalmologists 2022

PURPOSE: To describe the anterior segment optical coherence tomography (AS-OCT) appearance of conjunctival papilloma and identify differentiating features from papilliform ocular surface squamous neoplasia (OSSN).

METHOD: A retrospective chart review of individuals clinically diagnosed with conjunctival papilloma ($n = 10$) or papilliform OSSN ($n = 10$) based on slit lamp features. Data on demographics, tumour characteristics, and primary treatment were collected. AS-OCT features were assessed including epithelial thickness and reflectivity, a corrugated epithelial surface, presence of an overhanging edge, presence of intrinsic spaces and posterior shadowing. Histopathology was available in 5 papilloma and 3 OSSN specimens.

RESULT: Overall, the majority of individuals in both groups were white males. OSSN lesions were more likely to involve the limbus (80% vs. 10%, $p = 0.005$) and the bulbar conjunctiva (100% vs. 20%, $p < 0.001$) compared to papillomas. On AS-OCT, maximum epithelial thickness was thicker in papilloma compared to OSSN (936 ± 533 vs. 637 ± 207 μm , $p = 0.009$). The feature that best differentiated papilloma from OSSN was an overhanging edge (100% vs. 0%, $p < 0.001$), where the epithelial lesion was seen on top of underlying normal epithelium. Other features more common in papilloma compared to OSSN included a corrugated epithelial surface (70% vs. 10%, $p = 0.02$), the presence of intrinsic spaces (100% vs. 50%, $p = 0.03$), and posterior shadowing (100% vs. 40%, $p = 0.01$).

CONCLUSION: AS-OCT shows differentiating features between papilloma and OSSN with an overhanging edge as a distinctive AS-OCT feature of papilloma.

Eye (2023) 37:995–1001; <https://doi.org/10.1038/s41433-022-02309-7>

INTRODUCTION

Conjunctival papilloma represents a benign epithelial-derived tumour of the ocular surface, while ocular surface squamous neoplasia (OSSN) is known as its malignant counterpart. Both tumours have distinct clinical features. A conjunctival papilloma typically presents as an elevated cauliflower-like mass with multiple hairpin vessel loops [1]. The most common form is the pedunculated type with the presence of a pedicle being pathognomonic for papilloma. OSSN can have a variety of presentations with the major clinical appearances; gelatinous, leukoplakia, opalescent, and papilliform, described in the literature [2–4]. While in some cases, OSSN is easily recognizable on slit lamp examination, the diagnosis becomes more challenging when papilliform vessels are noted, as this vessel morphology can be shared between OSSN and papilloma.

In the early 2000s, the introduction of commercial anterior segment optical coherence tomography (AS-OCT) machines revolutionized the diagnostic approach to ocular surface tumours [4, 5]. The ability to visualize tumours from a cross-sectional

perspective allows AS-OCT to serve as an “optical-biopsy”. To date, there are a plethora of reports describing AS-OCT findings of benign and malignant ocular surface tumours with several lesions having characteristic features on AS-OCT [4, 6–13]. For example, characteristic features of OSSN include a thickened hyperreflective epithelium with abrupt transition from normal to abnormal epithelium. In fact, an epithelial thickness of ≥ 120 μm measured using the RTVue machine (Optovue, Fremont, CA), had a sensitivity of 100% and a specificity of 100% in differentiating OSSN from pterygia [14]. In addition, conjunctival nevi can be distinguished by their characteristic feature of cystic components within a subepithelial lesion [8, 14]. As such, the use of AS-OCT can aid the clinician to arrive at the correct diagnosis when characteristic features of a particular lesion are present. Missing from the literature, however, is a description of characteristic features of conjunctiva papilloma on AS-OCT. As this lesion can be clinically confused with papilliform OSSN, our study aimed to evaluate for specific AS-OCT findings that can aid the clinician in identifying this entity.

¹Bascom Palmer Eye Institute, Department of Ophthalmology University of Miami, Miami, FL, USA. ²Department of Ophthalmology, Faculty of Medicine, Srinakharinwirot University, Bangkok, Thailand. ³Florida Lions Ocular Pathology Laboratory, Miami, FL, USA. ⁴Department of Ophthalmology, Miami Veterans Administration Medical Center, Miami, FL, USA. ✉email: ckarp@med.miami.edu

Received: 28 February 2022 Revised: 24 July 2022 Accepted: 8 November 2022
Published online: 19 November 2022

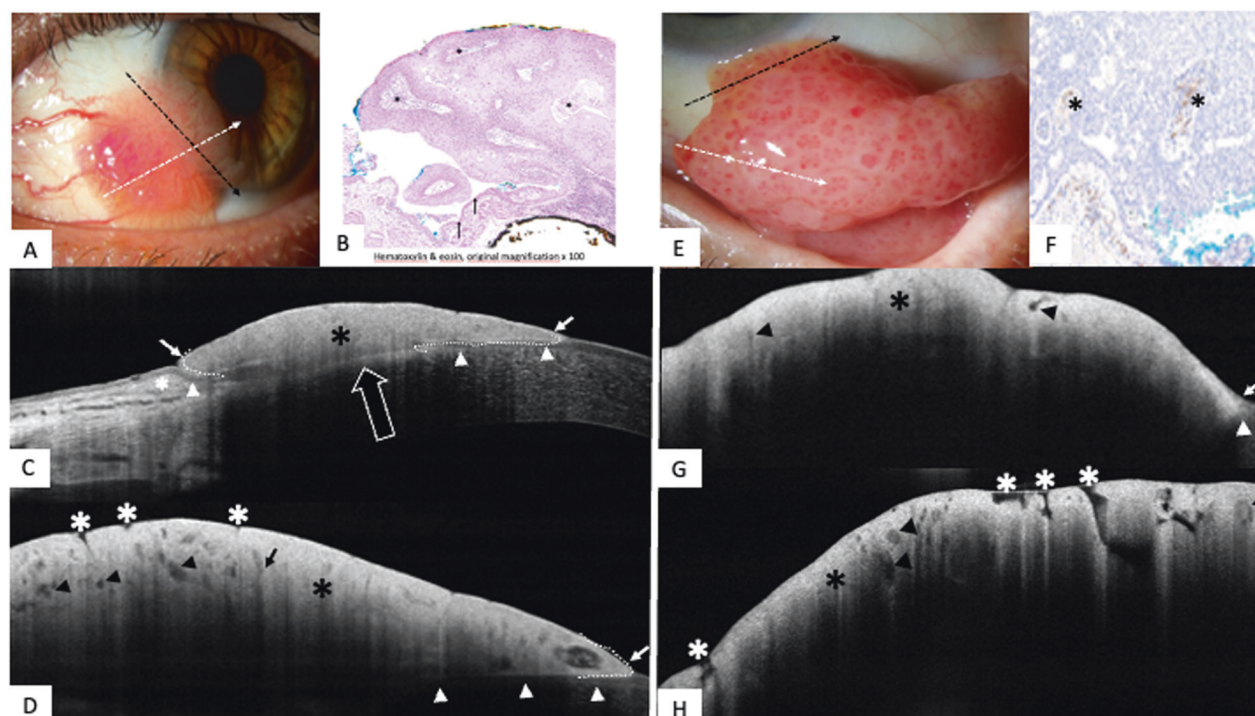


Fig. 1 Composite images of two conjunctival papilloma lesions. **A–D** A 48-year-old male with conjunctival papilloma in the left eye. Histopathologic examination from an incisional biopsy was consistent with conjunctival papilloma. He was treated with topical interferon alfa-2b eye drops until resolution. **A** Slit lamp photo demonstrates large circumscribed bulbar conjunctival lesion extending to cornea. Numerous intralesional papilliform vessels are noted. The black and white dotted arrow demonstrates the orientation of the anterior segment optical coherence tomography (AS-OCT) raster in **C** and **D**, respectively. **B** Histopathologic section of lesion in Fig. 1A discloses acanthotic epithelium overlying fibrovascular cores (asterisks) that overhangs the surrounding unremarkable epithelium (Haematoxylin & eosin, original magnification $\times 100$). **C** High-resolution AS-OCT image shows thickened hyperreflective epithelium (black asterisk). An underlying normal hyporefective epithelium is observed (white arrowheads) with overhanging edges (white arrows). The substantia propria and Tenon's is visible below the epithelium (white asterisk). White outlined arrow shows location of the presumed pedicle, dashed lines outline the wings of the stalked lesion. **D** High-resolution AS-OCT image shows thickened hyperreflective epithelium (black asterisk). The overhanging edges (white arrow and dotted line) with an underlying normal hyporefective epithelium is observed (white arrowheads). Numerous various size intrinsic spaces are seen (black arrowheads). Some spaces cast a shadowing effect (black arrows), obscuring details under the spaces. Corrugated surface of epithelium is also noted (white asterisks). **E–H** A 70-year-old female with conjunctival papilloma in the left eye. She underwent excisional biopsy with adjunctive cryotherapy. **E** Slit lamp photo demonstrates a large pedunculated lesion in inferior bulbar conjunctival involving the lower fornix with numerous hairpin vessels loops. The black and white dotted arrow demonstrates the orientation of the anterior segment optical coherence tomography (AS-OCT) raster in **G** and **H**, respectively. **F** Immunohistochemical stain for CD31 of lesion in Fig. 1E highlights the endothelial cells present in the fibrovascular cores of the lesion (asterisks) (CD31, original magnification $\times 200$). **G** High-resolution AS-OCT image shows thickened hyperreflective epithelium (black asterisk) and multiple intrinsic spaces (black arrowheads). The overhanging edge (arrow) with a normal underlying epithelium (white arrowhead) is noted. The visualization of the lesion base is obscured by posterior shadowing. **H** High-resolution AS-OCT image shows thickened hyperreflective epithelium (black asterisk) and multiple intrinsic spaces (black arrowheads). Corrugated surface of epithelium is also noted (white asterisks).

METHODS

This retrospective study was approved by the University of Miami Institutional Review Boards and was conducted in agreement with the principles of the Declaration of Helsinki and was compliant with the Health Insurance Portability and Accountability Act. An electronic database search of individuals diagnosed with conjunctival papilloma and individuals diagnosed with OSSN with a papilliform appearance from 2013 to 2021 was performed. We selected 10 patients with conjunctival papilloma and 10 patients with conjunctival papilliform ocular surface neoplasia for comparison. The diagnoses of conjunctival papilloma and papilliform OSSN were made by clinical examination by two ocular surface oncology specialists (AG and CLK). Diagnostic features of a conjunctival papilloma included the presence of a tumour peduncle and/or a floppy, mobile edge, together with multipin hairpin vessel loops. On the other hand, diagnostic features for a papilliform OSSN included the absence of a tumour peduncle with the lesion an integrated part of conjunctiva throughout, along with other features such as a gelatinous or leukoplakic component. Of note, conjunctival biopsy was not routinely performed due to the fear of possible viral spreading and extension of the lesion.

All individuals underwent slit lamp examination and AS-OCT imaging on their initial visit. Data on demographics, tumour characteristics (laterality,

appearance, number of tumours, tumour location, associated features; feeder vessel, intrinsic vascularity), AS-OCT imaging, and primary treatment were obtained.

AS-OCT imaging was performed with two spectral-domain OCT machines, Optovue RTVue (Fremont, CA) and Optovue Avanti (Fremont, CA), by two experienced ophthalmic technicians. The Optovue RTVue has an axial resolution of $5\ \mu\text{m}$, transverse resolution of $8\ \mu\text{m}$, and a scanning speed of 26,000 A-scans per second. The Optovue Avanti has an axial resolution of $5\ \mu\text{m}$, transverse resolution of $15\ \mu\text{m}$, scanning speed of 70,000 A-scans per second. Both machines use 840 nm wavelength light. Each lesion was scanned in a raster fashion (8 mm scanned length). Images were reviewed by the two senior authors (AG and CLK). Epithelial thickness was measured at the location with the thickest epithelium and a visible posterior border.

In addition, images were examined for qualitative features, all graded as absent or present that included [1] epithelial hyperreflectivity defined as an increased whiteness compared to normal tissue in the same location [2], corrugated epithelial surface (defined as a serrated-like appearance of the epithelial surface) [3], overhanging edge (defined as an area of thickened epithelial hyperreflectivity over the normal epithelium at the lesion edge) [4], intrinsic space (s) defined as circular, oval, or tubular hypo or hyper-reflective areas within an area of epithelial hyperreflectivity [5]. posterior

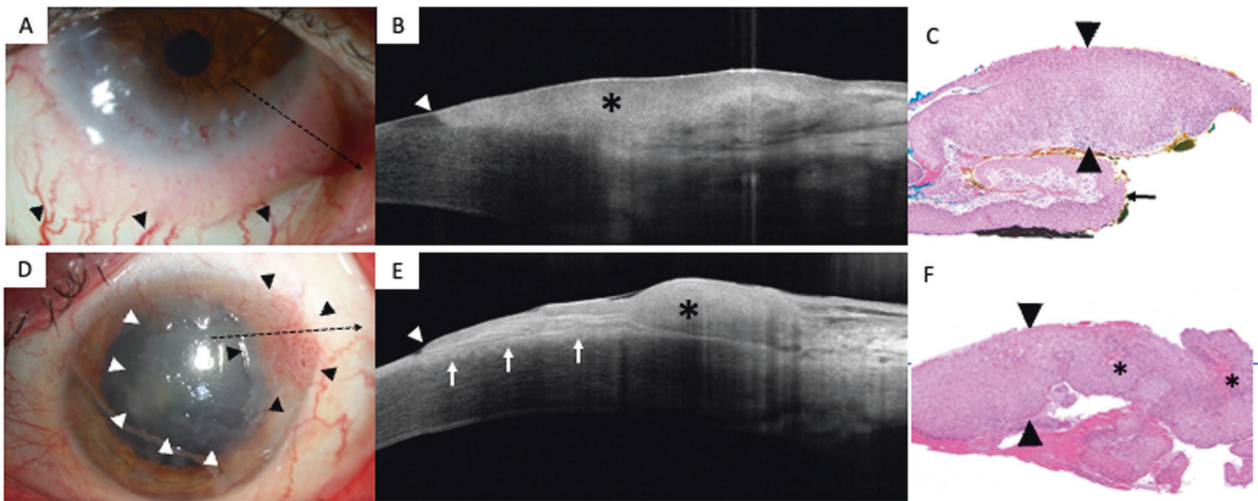


Fig. 2 Composite images of two ocular surface squamous neoplasia lesions. **A–C** A 65-year-old female with OSSN in the left eye. After failing topical 5FU, IFN and MMC eye drop, she underwent excisional biopsy with cryotherapy and MMC application. **A** Slit lamp photo demonstrates inferior circum-limbal papilliform lesion involving cornea. Feeder vessels were seen (arrowheads). The black dotted arrow demonstrates the orientation of the anterior segment optical coherence tomography (AS-OCT) raster in **B**. **B** High-resolution AS-OCT image shows thickened hyperreflective epithelium (asterisk) with abrupt transition (arrowhead). **C** Histopathologic examination of lesion in Fig. 1A discloses faulty epithelial maturational sequencing that extends up to full thickness (between arrowheads) with foci of pleomorphic and hyperchromatic nuclei. No invasion is identified in the available sections. A transition between unremarkable and neoplastic epithelium is present (arrow) (Haematoxylin & eosin, original magnification x 100). **D–F** A 58-year-old male with corneal scar from previous HSV and OSSN in the left eye. Histopathologic result from incisional biopsy was consistent with OSSN. He was treated with topical 5-fluorouracil eye drops. **D** Slit lamp image shows a mixed papilliform and gelatinous lesion on the supero-temporal limbal area (black arrowheads). A diffuse corneal scar was also noted (white arrowheads). The black dotted arrow demonstrates the orientation of the anterior segment optical coherence tomography (AS-OCT) raster. **E** High-resolution AS-OCT image shows thickened hyperreflective epithelium (asterisk) with an abrupt transition (arrowhead). Hyperreflectivity on the anterior corneal stroma is consistent with his HSV corneal scar (arrows). **F** Histopathologic examination of lesion in Fig. 1D discloses faulty epithelial maturational sequencing extending up to full thickness (between arrowheads) with foci of pleomorphic and hyperchromatic nuclei. Prominent fibrovascular cores are present in the epithelium (asterisk). No invasion is identified in the available sections. (Haematoxylin & eosin, original magnification x 100).

shadowing (defined as hyporeflexivity posterior to the area of hyperreflectivity leading to poor visualization in larger lesions), and [6] abrupt transition (defined as the transition between abnormal hyperreflective epithelium to normal epithelium). Examples of these features are presented in Figs. 1 and 2.

In our series, a large portion were treated medically, and incisional biopsy of a possible viral papilloma was avoided in classic cases to prevent possible viral seeding. Thus 5 of the 10 individuals with papilloma and 3 of the 10 individuals with OSSN, a confirmatory histopathologic diagnosis was available. Several pathologic staining methods were utilized in the available specimens that helped correlate histopathologic to OCT findings. Staining methods utilized included [1] haematoxylin & eosin (H&E) [2], alcian blue (to identify mucopolysaccharide), and [3] immunohistochemistry (IHC) for CD31 (clone 1A10; Leica, Buffalo Grove, IL; to identify vascular endothelium).

IBM SPSS Statistics for Macintosh, Version 27.0 (IBM Inc., IL, USA) was utilized for the statistical analysis. Descriptive statistics were used to summarize demographics as well as tumour characteristics. Continuous variables were compared with independent students' T-test. Categorical variables were compared with Chi-square methodology. A p -value <0.05 was considered statistically significant.

RESULTS

Study population and clinical features of conjunctival papilloma and OSSN

Twenty eyes of twenty patients were included in this study. Baseline demographics and tumour characteristics of the two groups are shown in Table 1. Overall, the majority of individuals in each group were male, white, and non-Hispanic. Individuals with OSSN were older than their papilloma counterparts (69 vs. 58 years, $p = 0.01$).

OSSN lesions were more likely to involve the limbus (80% vs. 10%, $p = 0.005$) or the bulbar conjunctiva (100% vs. 20%,

$p < 0.001$) compared to papillomas. Temporal lesion location was more common in OSSN than papilloma (50% vs. 0%, $p = 0.03$). All papilloma and none of the OSSN lesions had a mobile edge while feeder vessels (100% vs. 20%, $p < 0.001$) and an opalescent appearance (70% vs. 0%, $p = 0.003$) were seen more often in OSSN as opposed to papilloma.

Treatment approaches for conjunctival papilloma and OSSN

In 3 individuals, the papilloma was treated with excisional biopsy and cryotherapy (1 with intraoperative adjunctive mitomycin C (MMC), 1 with intraoperative interferon alfa-2b (IFN) injection). In the remaining 7 individuals, the papilloma was treated medically (3 with topical interferon, IFN), 2 with topical 5-fluorouracil (5FU), 1 with oral cimetidine, 1 with the off-label use of human papillomavirus vaccine intramuscular injection (Gardasil-9, Merck, Durham, North Carolina). This was based on our and other experience using the HPV vaccine for therapeutic purposes [15–17]. In all individuals, OSSN was treated topically (2 with IFN eye drops and 8 with 5FU eye drops).

Regarding treatment outcomes, the papilloma completely resolved in 3 individuals after excisional biopsy. Three individuals (1 IFN and 2 5FU) had reduction in the lesions and were subsequently observed off treatment as their lesion was asymptomatic, 2 (IFN) had chemoreduction and then underwent excisional biopsy, 1 (oral cimetidine) was lost to follow up, and 1 (HPV vaccine) had complete resolution following 2 IM injections of the HPV vaccine. In the OSSN group, 2 lesions treated with IFN and 7 treated with 5FU completely resolved with therapy. In one individual, the lesion failed to respond to 5FU and also failed subsequent IFN and MMC. This patient underwent excision with cryotherapy with resolution of OSSN.

Table 1. Patients' demographics and clinical characteristic of tumours in each group.

	Papilloma	Papilliform OSSN	p-value
Demographics and co-morbidities			
Age, mean, [SD], (range)	58.3, [14.23], (20–70)	68.8, [11.5], (47–82)	0.01
Gender, Male, %(n)	70% (7)	60% (6)	1
Race			
White, %(n)	90% (9)	90% (9)	1
Black, %(n)	10% (1)	10% (1)	
Ethnicity, Non-Hispanic, %(n)	70% (7)	60% (6)	1
Immunocompromised status, %(n)	10% (1)	10% (1)	1
Tumour information			
Eye, OD, % (n)	30% (3)	50% (5)	0.65
Number of tumours per eye mean, [SD], (range)	1.7, [1.1], (1–4)	1, [0], (1)	0.07
Location of tumour epicentre			
Superior	10% (1)	40% (4)	0.3
Inferior	70% (7)	50% (5)	0.65
Temporal	0%	50% (5)	0.03
Nasal	40% (4)	80% (8)	0.17
Location of tumour			
Limbus	10% (1)	80% (8)	0.005
Bulbar conjunctiva	20% (3)	100% (10)	<0.001
Fornix	40% (4)	10% (1)	0.3
Tarsal conjunctiva	30% (3)	10% (1)	0.58
Caruncle and plica	30% (3)	20% (2)	1
Lid margin	10% (1)	0%	1
Histopathologic confirmation	50% (5)	30% (3)	0.65
Primary treatment given			
Excisional biopsy	30% (3)	0	0.21
Medical therapy	70% (7)	100% (10)	

AS-OCT characteristics of conjunctival papilloma and OSSN

Overall, several features differentiated papilloma from OSSN. First, papilloma had a thicker mean epithelial thickness compared to OSSN (936 ± 533 vs. 637 ± 207 μm , $p = 0.009$). Of the AS-OCT features, an overhanging edge was most specific to papilloma, meaning that tumour was seen overlying adjacent normal epithelium. This “mushrooming” was found in all papilloma and no OSSN lesions. Other features more common in papilloma compared to OSSN included a corrugated epithelial surface (70% vs. 10%, $p = 0.02$), one or more intrinsic spaces (100% vs. 50%, $p = 0.03$), and posterior shadowing (100% vs. 40%, $p = 0.01$). On the other hand, an abrupt transition from normal to abnormal epithelium was seen exclusively in the OSSN group (100% vs. 0%, $p < 0.001$). Table 2 summarizes the frequencies of clinical and AS-OCT parameters in the papilloma and papilliform OSSN groups.

Histopathologic correlations of AS-OCT findings in conjunctival papilloma and OSSN

Correlation among clinical, AS-OCT, and histologic findings of papilloma are described in Table 3. The findings noted when examining papilloma clinically and histopathologically likely explain the noted AS-OCT features. First, the elevated mass with irregular surface seen clinically was observed as a thickened hyperreflective epithelium with a corrugated surface on AS-OCT. This correlated with our finding that conjunctival papilloma is histopathologically composed of fibrovascular cores draped in multilayered, nonkeratinized squamous epithelial cells attached to a pedicle demonstrated on H&E (Fig. 1B, Supplementary Fig. 1A). Second, the clinically noted mobile edge of a papilloma manifests

as an overhanging edge of abnormally thickened hyperreflective epithelium folded over normal epithelium on AS-OCT (Fig. 1C, G) and mushroom-shaped acanthotic epithelium overlying fibrovascular cores on histopathology (Fig. 1B, F, Supplementary Figs. 1 and 2). Third, the papilliform vessels may explain the intrinsic spaces of various shapes and sizes noted on AS-OCT and were seen as vascular lumen on H&E which was confirmed by CD31 (Fig. 1F, Supplementary Fig. 2). Moreover, we identified another potential aetiology of the noted intrinsic spaces from histopathology, namely proteinaceous cystic spaces, but were unable to identify these clinically nor differentiate them from vascular lumen on AS-OCT. Lastly, posterior shadowing (Fig. 1D, G) is an optical phenomenon explained by the blockage of light transmission by acanthotic epithelium, vascular lumens, or proteinaceous cystic spaces.

OSSN has in common a feature of papilloma on histology namely acanthotic epithelium. A main differentiator between OSSN and papilloma is the presence of nuclear abnormalities on histology including abnormal nuclear chromatin, prominent nucleoli, mitotic activity, and dyskeratosis. However, nuclear abnormalities cannot be detected clinically or on AS-OCT. A key feature of OSSN is the abrupt transition from normal to abnormal epithelium. This is seen pathologically and visible on AS-OCT.

The overlap in AS-OCT features between papilloma and OSSN can be explained by histopathologic similarities (Fig. 2). Both tumours demonstrate acanthotic epithelium, manifesting as thickened hyperreflective epithelium. However, the epithelium was thicker and overall, more heterogenous (due to the presence of intrinsic holes and a corrugated surface) in papilloma compared

Table 2. Clinical morphology and anterior segment optical coherence tomography (AS-OCT) characteristic features of papilloma and papilliform ocular surface squamous neoplasia (OSSN).

	Papilloma	Papilliform OSSN	p-value
Clinical features			
Elevation	100%(10)	100%(10)	
Papilliform vessels	100%(10)	100%(10)	
Mobile edge	100%(10)	0	<0.001
Feeder vessels	20%(2)	100%(10)	<0.001
Opalescence	0	70%(7)	0.003
AS-OCT features			
Epithelial thickness in um, mean, [SD], (range)	936, [533], (291–1,865)	637, [207], (427–1,143)	0.009
Epithelial hyperreflectivity	100%(10)	100%(10)	
Corrugated epithelial surface	70%(7)	10%(1)	0.02
Overhanging edge	100%(10)	0	<0.001
Intrinsic spaces	100%(10)	50%(5)	0.03
Posterior shadowing	100%(10)	40%(4)	0.01
Abrupt transition	0	100%(10)	<0.001

Table 3. Correlation between AS-OCT and histologic structures in conjunctival papilloma.

Clinical findings	AS-OCT findings	Histopathologic findings
Elevation with irregular surface	Thickened hyperreflective epithelium with corrugated surface	Acanthotic epithelium with overlying variable indentation of the surface epithelium
Mobile edge	Overhanging edge of abnormal epithelium over normal epithelium	Acanthotic epithelium that overhangs the surrounding unremarkable epithelium
Papilliform vessels ^a	Intrinsic spaces/holes	Cross sectional view of fibrovascular cores or proteinaceous cystic spaces
None	Posterior shadowing	None but could be explain by the blockage of light transmission caused by acanthotic epithelium, vascular lumen or proteinaceous cystic spaces

^aPapilliform vessels were seen as spaces in AS-OCT and correlated with fibrovascular cores in histology. Proteinaceous cystic space was not observed clinically nor differentiate in the AS-OCT image.

to OSSN. OSSN also infrequently had intrinsic holes, but they were smaller and less numerous than in papilloma. All cases of OSSN had an abrupt transition from normal to abnormal.

DISCUSSION

In summary, we retrospectively reviewed AS-OCT images of conjunctival papillomas and papilliform OSSN and noted specific differentiating features between the two lesions. Mirroring what is seen clinically, an overhanging edge on AS-OCT most distinctly differentiated papilloma from papilliform OSSN with 100% sensitivity and specificity. In addition, other features more commonly seen on AS-OCT in papilloma compared to OSSN included a thicker hyperreflective epithelium and the presence of a corrugated epithelial surface, intrinsic spaces, and posterior shadowing.

In one of our previous analyses and publication of AS-OCT findings of conjunctival papilloma [1], the presence of thickened hyperreflective epithelium with a dome-shaped or lobulated configuration was also noted. In our current study, we evaluated more papillomas and also compared them to OSSN lesions. We further found that the epithelial thickness in papilloma was greater than that in OSSN, with a more heterogeneous appearance driven by a corrugated surface, presence of intrinsic spaces, and posterior shadowing, features not detected in the prior report [1].

Our findings on OSSN AS-OCT features mirror that of our previous work, with a thickened hyperreflective epithelium with

an abrupt transition from normal to abnormal epithelium noted in all cases [4, 6, 9]. In this study, we demonstrate that papilliform OSSN has the same AS-OCT features as other OSSN sub-types.

When examining histopathologic correlates, we identified several features on histopathology that likely explained the AS-OCT findings. First, the thickened hyperreflective epithelium with a corrugated surface was identified in histology as acanthotic epithelium. An overhanging edge, the most specific AS-OCT features of papilloma, was noted histologically to be a fold of acanthotic epithelium over the normal conjunctival epithelium. Intrinsic spaces likely represent cross-sectional views of cystic/luminal spaces of either vascular (lumen) or non-vascular aetiology (proteinaceous-filled cysts) which were both seen on histology. Unfortunately, we could not differentiate between these two possibilities on AS-OCT. As above, posterior shadowing does not represent a histologic structure but is an observed optical phenomenon of blockage of light transmission from a thick lesion. However, other features, beyond thickness, can induce posterior shadowing such as pigmentation (as seen in conjunctival melanoma and nevus), and calcification (as seen in band keratopathy) [8, 18].

Our findings need to be considered in light of our study limitations which included a limited number of patients. Furthermore, histopathologic confirmation was not available for all individuals. In individuals with papilloma, an incisional biopsy is typically not performed for fear of seeding virus and disseminating the lesion. In OSSN, given our previous work on the utility of AS-OCT, we have shifted away from the routine

biopsy in patients with classic features [19–21]. Instead, we reserve biopsy for individuals with ambiguous lesions, those not responding to therapy, or those who elect to have an excisional biopsy of their lesion. Moreover, AS-OCT technical limitations need to be considered. For example, measurement of epithelial thickness was difficult in some cases due to posterior shadowing obscuring the posterior border of the lesion. As a result, the thickness measured in both the OSSN and papillomas may be an underestimation of the true epithelial thickness, as thicker areas caused shadowing and could not be fully measured.

Despite these limitations, our study examined AS-OCT features of conjunctival papilloma and found several that differentiated papilloma from OSSN. Foremost, an overhanging, “mushroom” like edge was the key distinctive feature of papilloma that was not seen in OSSN. In addition, a thickened hyperreflective epithelium, corrugated surface, and intrinsic spaces with heterogenous appearance were all more common in papilloma as compared to OSSN. None of the papilloma lesions had an abrupt transition from normal to abnormal epithelium as seen in OSSN. Our study is the first to compare the characteristics of AS-OCT between OSSN and papilloma. These findings can be added to the armamentarium of AS-OCT features that can help clinicians diagnose ocular surface lesions. However, as AS-OCT has limitations, when clinical examination and AS-OCT findings are ambiguous, a biopsy is needed to definitively diagnose a lesion.

Summary Table

What was known before

- Conjunctival ocular surface squamous neoplasia has characteristic features of thickened hyper-reflective epithelium with abrupt transition from normal to abnormal epithelium.
- Neither previous report of AS-OCT findings in conjunctival papilloma nor the comparison between OSSN and papilloma are present in the literature.

What this study adds

- AS-OCT characteristics of papilloma are thickened hyperreflective epithelium with overhanging edge, corrugated epithelial surface, the presence of intrinsic spaces.
- AS-OCT shows differentiating features between papilloma and OSSN with an overhanging edge as a distinctive AS-OCT feature of papilloma.

DATA AVAILABILITY

The datasets generated during and/or analysed during the current study are available from the corresponding author on reasonable request.

REFERENCES

1. Theotoka D, Morkin MI, Galor A, Karp CL. Update on diagnosis and management of Conjunctival Papilloma. *Eye Vis.* 2019;6:18.
2. Lee GA, Hirst LW. Ocular surface squamous neoplasia. *Surv Ophthalmol.* 1995;39:429–50.
3. Shields CL, Shields JA. Tumors of the conjunctiva and cornea. *Surv Ophthalmol.* 2004;49:3–24.
4. Thomas BJ, Galor A, Nanji AA, El Sayyad F, Wang J, Dubovy SR, et al. Ultra high-resolution anterior segment optical coherence tomography in the diagnosis and management of ocular surface squamous neoplasia. *Ocul Surf.* 2014; 12:46–58.
5. Ang M, Baskaran M, Werkmeister RM, Chua J, Schmidl D, Aranha dos Santos V, et al. Anterior segment optical coherence tomography. *Prog Retinal Eye Res.* 2018;66:132–56.

6. Atallah M, Joag M, Galor A, Amescua G, Nanji A, Wang J, et al. Role of high-resolution optical coherence tomography in diagnosing ocular surface squamous neoplasia with coexisting ocular surface diseases. *Ocul Surf.* 2017;15:688–95.
7. Kaliki S, Maniar A, Jakati S, Mishra DK. Anterior segment optical coherence tomography features of pseudoepitheliomatous hyperplasia of the ocular surface: a study of 9 lesions. *Int Ophthalmol.* 2021;41:113–9.
8. Shields CL, Belinsky I, Romanelli-Gobbi M, Guzman JM, Mazzuca D, Green WR, et al. Anterior segment optical coherence tomography of conjunctival nevus. *Ophthalmology.* 2011;118:915–9.
9. Shousha MA, Karp CL, Perez VL, Hoffmann R, Ventura R, Chang V, et al. Diagnosis and management of conjunctival and corneal intraepithelial neoplasia using ultra high-resolution optical coherence tomography. *Ophthalmology.* 2011;118:1531–7.
10. Venkateswaran N, Mercado C, Tran AQ, Garcia A, Diaz PFM, Dubovy SR, et al. The use of high-resolution anterior segment optical coherence tomography for the characterization of conjunctival lymphoma, conjunctival amyloidosis and benign reactive lymphoid hyperplasia. *Eye Vis.* 2019;6:17.
11. Vempuluru VS, Jakati S, Godbole A, Mishra DK, Mohamed A, Kaliki S. Spectrum of AS-OCT features of ocular surface tumors and correlation of clinico-tomographic features with histopathology: a study of 70 lesions. *Int Ophthalmol.* 2021;41:3571–86.
12. Han SB, Liu YC, Noriega KM, Mehta JS. Applications of anterior segment optical coherence Tomography in cornea and ocular surface diseases. *J Ophthalmol.* 2016;2016:4971572.
13. Kievla JZ, Karp CL, Shousha MA, Galor A, Hoffman RA, Dubovy SR, et al. Ultra-high resolution optical coherence tomography for differentiation of ocular surface squamous neoplasia and pterygia. *Ophthalmology.* 2012;119:481–6.
14. Nanji AA, Sayyad FE, Galor A, Dubovy S, Karp CL. High-resolution optical coherence tomography as an adjunctive tool in the diagnosis of corneal and conjunctival pathology. *Ocul Surf.* 2015;13:226–35.
15. Nichols AJ, Gonzalez A, Clark ES, Khan WN, Rosen AC, Guzman W, et al. Combined systemic and intratumoral administration of human papillomavirus vaccine to treat multiple cutaneous basaloid squamous cell carcinomas. *JAMA Dermatol.* 2018;154:927–30.
16. Bossart S, Gabutti MP, Seyed Jafari SM, Hunger RE. Nonavalent human papillomavirus vaccination as alternative treatment for genital warts. *Dermatol Ther.* 2020;33:e13771.
17. Sripawadkul W, AlBayyat G, Galor A, Wylegala A, Nichols AJ, Ioannides T, et al. Resolution of a presumed conjunctival papilloma after therapeutic treatment with the human papillomavirus vaccine. *JAMA Ophthalmol.* 2022;140:434–5.
18. Venkateswaran N, Galor A, Wang J, Karp CL. Optical coherence tomography for ocular surface and corneal diseases: a review. *Eye Vis.* 2018;5:13.
19. Nanji AA, Moon CS, Galor A, Sein J, Oellers P, Karp CL. Surgical versus medical treatment of ocular surface squamous neoplasia: a comparison of recurrences and complications. *Ophthalmology.* 2014;121:994–1000.
20. Joag MG, Sise A, Murillo JC, Sayed-Ahmed IO, Wong JR, Mercado C, et al. Topical 5-Fluorouracil 1% as primary treatment for ocular surface squamous neoplasia. *Ophthalmology.* 2016;123:1442–8.
21. Venkateswaran N, Mercado C, Galor A, Karp CL. Comparison of Topical 5-Fluorouracil and Interferon Alfa-2b as primary treatment modalities for ocular surface squamous neoplasia. *Am J Ophthalmol.* 2019;199:216–22.

AUTHOR CONTRIBUTIONS

WS: conception of the study, data acquisition, analysis and draughting the manuscript. RK and VT: data acquisition. MZ: data acquisition and draughting the manuscript. SD: interpreting data. AG: conception of the study, data analysis, critical revision of the manuscript. CK: conception of the study, data analysis, final approval of the manuscript.

FUNDING

NIH Center Core Grant P30EY014801, RPB Unrestricted Award and Career Development Awards, Dr. Ronald and Alicia Lepke Grant, The Lee and Claire Hager Grant, The H. Scott Huizenga Grant, The Grant and Diana Stanton-Thornbrough Grant, The Robert Baer Family Grant, The Emilyn Page and Mark Feldberg Grant, The Jose Ferreira de Melo Grant, The Robert and Virginia Farr Grant, The Richard and Kathy Lesser Grant, The Michele and Ted Kaplan Grant, The Calvin and Flavia Oak Foundation, The Honorable A. Jay Cristol Grant, The Christian Kathke Grant, The Mr. and Mrs. Irwin Friedman Grant, The Roberto and Antonia Family Grant, The Carol Soffer Grant, and The Richard Azar Family Grant (Dr. Karp-institutional grants), The Department of Veterans Affairs, Veterans Health Administration, Office of Research and Development, Clinical Sciences R&D (CSR) I01 CX002015 (Dr. Galor) and Biomedical Laboratory R&D (BLRD) Service I01 BX004893 (Dr. Galor), Department of Defense Gulf War Illness Research Program (GWIRP) W81XWH-20-1-0579 (Dr. Galor)

and Vision Research Program (VRP) W81XWH-20-1-0820 (Dr. Galor), National Eye Institute R01EY026174 (Dr. Galor) and R61EY032468 (Dr. Galor), and Research to Prevent Blindness Unrestricted Grant (institutional).

COMPETING INTERESTS

The authors declare no competing interests.

ADDITIONAL INFORMATION

Supplementary information The online version contains supplementary material available at <https://doi.org/10.1038/s41433-022-02309-7>.

Correspondence and requests for materials should be addressed to Carol L. Karp.

Reprints and permission information is available at <http://www.nature.com/reprints>

Publisher's note Springer Nature remains neutral with regard to jurisdictional claims in published maps and institutional affiliations.

Springer Nature or its licensor (e.g. a society or other partner) holds exclusive rights to this article under a publishing agreement with the author(s) or other rightsholder(s); author self-archiving of the accepted manuscript version of this article is solely governed by the terms of such publishing agreement and applicable law.